

A Vision-based Nonlinear Decentralized Controller for Unmanned Vehicles

Omar A. A. Orqueda and Rafael Fierro
MARHES Laboratory
School of Electrical and Computer Engineering
Oklahoma State University
Stillwater, OK 74078-5032, USA
Email: {omar.orqueda, rfierro}@okstate.edu

Abstract— This paper presents a vision-based control strategy for decentralized stabilization of *unmanned vehicle* (UV) formations. The key point of the algorithm is that it only requires knowledge of the leader-follower relative distance and bearing. The approach is based on an output feedback controller that uses a high-gain observer to estimate derivatives of UV's relative positions. Both data are measured using a pan-controlled camera on-board the following robot which eliminates sensitivity to information flow among vehicles. A Lyapunov stability analysis guarantees that the closed-loop system is stable and the formation error can be made arbitrarily small. A virtual environment and a vision system are used to validate the proposed methodology.

I. INTRODUCTION

The problem of controlling groups of UVs has gained interest in recent years motivated by several exciting applications, such as automated transportation, spacecraft interferometry, mitigation of natural and man-made disasters, surveillance, mapping, border patrol, and search and rescue. In these applications, a system composed of multiple cooperative robots is desirable because of its size, cost, and flexibility [1].

Research on multi-vehicle system coordination has been focused both on *centralized* and *decentralized* control strategies. Centralized control strategies have the advantage of being able to reach a global optimum solution for tasks such as path planning and reconfiguration [2], [3], [4]. However, these algorithms become infeasible when the number of vehicles and constraints increase, hindering their implementation in real-time. On the other hand, decentralized control approaches only require local information and can effectively achieve coordination behaviors as the ones observed in flocks of birds or schools of fish. In these behaviors, individuals do not use explicit communication but local sensing in order to maintain coherent formations or coordinate motions, even when they have to move around obstacles or avoid predators [5], [6], [7].

Many approaches for solving multi-robot coordination problems reduce to a single-agent control problem by assuming that global communication is available. However, a coordination mechanism that does not rely on global information sharing ensures flexibility and mission safety because reference trajectories and mission objectives should not be shared among all agents but some leaders [8]. Of course, this poses a challenge on the design of the formation controllers.

In the last few years, several motion coordination algorithms have been proposed. In [9], authors developed an omnidirectional visual servoing and motion segmentation-based formation control algorithm. Vision-based formation controllers are described in [10]. The algorithms are based on input-output linearization and require the estimation of the leader-follower relative angle and the leader's linear and angular velocities. Chen *et al.* [8] propose a decentralized control architecture that employs relative position and velocities between a robot and its leader. In [6], a vision-based distributed coordination approach based on nearest-neighbor interactions is developed. The approach assumes that robots move with constant speed and achieve flocking after certain time. In general, flocking algorithms do not maintain a rigid formation shape. Such formation maintenance is critical in applications like cooperative payload transport [11] and cooperative object pushing [12].

In this paper, we present a decentralized output feedback controller based on monocular vision information. A high-gain observer is used to estimate the derivatives of the relative position between a robot and its leader. The algorithm eliminates the need of inter-vehicle communication, increasing the reliability of the overall system.

The rest of the paper is organized as follows. In Section II, we review definitions on formations. The problem statement is given in Section III. Section IV analyzes our decentralized formation control algorithm. Section V provides numerical simulations in a virtual environment. Finally, we present our concluding remarks and future work in Section VI.

II. DEFINITIONS AND PRELIMINARY REMARKS

This section reviews some concepts on formations. For a detailed treatment and definitions on graphs see [13], [14].

A. Mathematical Model

Let us consider a multi-robot system composed of N_a agents modeled as unicycle-type velocity-controlled vehicles with the kinematic model of the i -th robot given by¹

$$\dot{q}_i(t) = \begin{bmatrix} c_{\theta_i(t)} & 0 \\ s_{\theta_i(t)} & 0 \\ 0 & 1 \end{bmatrix} u_i(t), \quad (1)$$

¹Note that other system models can be adapted to this framework.

where $q_i(t) := [x_i(t), y_i(t), \theta_i(t)]^T \in SE(2)$, $u_i(t) := [v_i(t), \omega_i(t)]^T \in \mathcal{U}_i \subseteq \mathbb{R}^2$ is the control vector given by the linear and the angular velocities, \mathcal{U}_i is a compact set of admissible inputs, $c_{\theta_i}(t) := \cos \theta_i(t)$, and $s_{\theta_i}(t) := \sin \theta_i(t)$.

Let the Euclidean distance $\ell_{ij}(t) \in \mathbb{R}_{\geq 0}$ and the bearing $\psi_{ij}(t) \in (-\pi, \pi]$ between robots i and j be defined as

$$\ell_{ij}(t) := \sqrt{(x_i - x_j)^2 + (y_i - y_j)^2}, \quad (2)$$

$$\psi_{ij}(t) := \pi + \zeta_{ij}(t) - \theta_i(t), \quad (3)$$

with $\zeta_{ij}(t) = \text{atan2}(y_i - y_j, x_i - x_j)$, as shown in Figure 1.

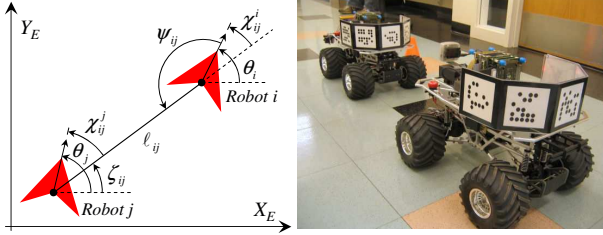


Fig. 1. Formation geometry.

B. Formations

Definition 1: A formation is a network of vehicles interconnected via their controller specifications that dictate the relationship each agent must maintain with respect to its leader. The interconnections between agents are modeled as edges in a directed acyclic graph, labeled by a given relationship [14].

Definition 2: A formation control graph $\mathcal{G} = (\mathcal{V}, \mathcal{E}, \mathcal{S})$ is a directed acyclic graph consisting of the following:

- A finite set $\mathcal{V} = (v_1, \dots, v_N)$ of N vertices and a map assigning to each vertex v_i a control system (1).
- An edge set $\mathcal{E} \subset \mathcal{V} \times \mathcal{V}$ encoding leader-follower relationships between agents. The ordered pair $(v_i, v_j) := e_{ij}$ belongs to \mathcal{E} if u_j depends on the state of agent i , q_i .
- A collection $\mathcal{S} = \{s_{ij}\}$ of node specifications defining control objectives, or *set points*, for each node j , such that $(v_i, v_j), (v_k, v_j) \in \mathcal{E}$ for some $v_i, v_j, v_k \in \mathcal{V}$.

III. PROBLEM STATEMENT

The coordination controller presented in this paper is based on the distance and bearing between the robot j and its leader i . Then, let the node specification of robot j , $s_{ij}(t) \in \mathbb{R}^2$, be given by

$$s_{ij}(t) := [\ell_{ij}(t), \psi_{ij}(t)]^T. \quad (4)$$

Taking the time derivative of (4) we obtain

$$\dot{s}_{ij}(t) = \begin{bmatrix} \dot{\ell}_{ij}(t) \\ \dot{\psi}_{ij}(t) \end{bmatrix} = -\varphi_{ij}(s_{ij}) v_j(t) - \varphi_{ij}^u(s_{ij}) u_i(t), \quad (5)$$

where $\varphi_{ij}(s_{ij}) \in \mathbb{R}^2$ and $\varphi_{ij}^u(s_{ij}) \in \mathbb{R}^{2 \times 2}$ are given by

$$\varphi_{ij}(s_{ij}) := \begin{bmatrix} -c_{\gamma_{ij}} \\ \frac{s_{\gamma_{ij}}}{\ell_{ij}} \end{bmatrix}, \quad \varphi_{ij}^u(s_{ij}) := \begin{bmatrix} c_{\psi_{ij}} & 0 \\ -\frac{s_{\psi_{ij}}}{\ell_{ij}} & 1 \end{bmatrix}, \quad (6)$$

where $\gamma_{ij}(t) := \pi + \zeta_{ij}(t) - \theta_j(t)$. Taking the time derivative of (5), the following equation is obtained

$$\ddot{s}_{ij}(t) = \begin{bmatrix} \ddot{\ell}_{ij}(t) \\ \ddot{\psi}_{ij}(t) \end{bmatrix} = -g_{ij}(s_{ij}, v_j) \varpi_j(t) - g_{ij}^s(s_{ij}, v_j) \dot{s}_{ij}(t) - g_{ij}^v(s_{ij}, v_j) V_i(t), \quad (7)$$

with $g_{ij}, g_{ij}^s \in \mathbb{R}^{2 \times 2}$, and $g_{ij}^v \in \mathbb{R}^{2 \times 6}$ given by

$$g_{ij} := \begin{bmatrix} -\frac{c_{\gamma_{ij}}}{\ell_{ij}} & -\frac{v_j s_{\gamma_{ij}}}{\ell_{ij}} \\ \frac{s_{\gamma_{ij}}}{\ell_{ij}} & -\frac{v_j c_{\gamma_{ij}}}{\ell_{ij}} \end{bmatrix}, \quad g_{ij}^s := \begin{bmatrix} 0 & \frac{v_j s_{\gamma_{ij}}}{\ell_{ij}} \\ -\frac{v_j s_{\gamma_{ij}}}{\ell_{ij}^2} & \frac{v_j c_{\gamma_{ij}}}{\ell_{ij}} \end{bmatrix}, \quad (8)$$

$$g_{ij}^v := \begin{bmatrix} \frac{v_j s_{\gamma_{ij}} s_{\psi_{ij}}}{\ell_{ij}} & c_{\psi_{ij}} & -\frac{s_{\psi_{ij}}^2}{\ell_{ij}} & s_{\psi_{ij}} & v_j s_{\gamma_{ij}} & 0 \\ \frac{v_j s_{\gamma_{ij}} + \psi_{ij}}{\ell_{ij}^2} & \frac{s_{\psi_{ij}}}{\ell_{ij}} & -\frac{s_{\psi_{ij}}^2}{\ell_{ij}^2} & \frac{c_{\psi_{ij}}}{\ell_{ij}} & \frac{v_j c_{\gamma_{ij}}}{\ell_{ij}} & 1 \end{bmatrix}, \quad (9)$$

the vector $V_i(t) \in \mathbb{R}^6$ given by

$$V_i(t) := [v_i(t), \dot{v}_i(t), v_i^2(t), v_i(t)\omega_i(t), \omega_i(t), \dot{\omega}_i(t)]^T,$$

and the basic control vector $\varpi_j(t) \in \mathbb{R}^2$ defined as

$$\varpi_j(t) := [\dot{v}_j(t), \omega_j(t)]^T. \quad (10)$$

The matrix $g_{ij}(s_{ij}, v_j)$ in (8) is nonsingular if $v_j(t) \geq v_{\min} > 0$ and $\ell_{ij}(t) \geq \ell_{\min} > 0$, where ℓ_{\min} is the minimum distance required to avoid inter-robot collisions.

The objective is to design a control law $u_j(t)$, based on (10), that allows robot j to track its leader i with a desired specification $s_{ij}^d(t)$, assuming that robot i is stably tracking a desired trajectory $u_i^d(t) := [v_i^d(t), \omega_i^d(t)]^T$ such that $u_i^d(t), \dot{u}_i^d(t), \ddot{u}_i^d(t) \in \mathcal{L}_\infty$, and then $u_i(t), \dot{u}_i(t), \ddot{u}_i(t) \in \mathcal{L}_\infty$.

Let the specification error $e_{ij}(t) \in \mathbb{R}^2$ be defined as

$$e_{ij}(t) := s_{ij}^d(t) - s_{ij}(t). \quad (11)$$

Taking first and second time derivatives of (11) we have

$$\dot{e}_{ij}(t) = \dot{s}_{ij}^d(t) + \varphi_{ij}(s_{ij}) v_j(t) + \varphi_{ij}^u(s_{ij}) u_i(t), \quad (12)$$

$$\ddot{e}_{ij}(t) = g_{ij}(s_{ij}, v_j) \varpi_j(t) + \phi(\dot{s}_{ij}, s_{ij}, v_j) + g_{ij}^v(s_{ij}, v_j) V_i(t), \quad (13)$$

with

$$\phi(\dot{s}_{ij}, s_{ij}, v_j) := \ddot{s}_{ij}^d(t) + g_{ij}^s(s_{ij}, v_j) \dot{s}_{ij}(t). \quad (14)$$

Let the filtered error signal $r(t) \in \mathbb{R}^2$ be defined as

$$r(t) := \dot{e}_{ij}(t) + K e_{ij}(t), \quad (15)$$

where $K = \text{diag}(k_1, k_2) \in \mathbb{R}_{>0}^{2 \times 2}$ is a constant gain matrix. Differentiating (15) and using (12)-(13) yields

$$\dot{r}(t) = g_{ij}(s_{ij}, v_j) \varpi_j(t) + \phi(\dot{s}_{ij}, s_{ij}, v_j) + g_{ij}^v(s_{ij}, v_j) V_i(t) + K \dot{e}_{ij}(t). \quad (16)$$

The design of a controller for (16) can be made using three levels of information: The first level, and the most complex from the point of view of information flow, is given by the knowledge of the velocity and acceleration of the leader, the specification, and its derivative. The second level requires the knowledge of the specification and its derivative. Finally, the

third and simplest level from the information flow point of view, only requires the knowledge of the specification.

In the rest of this Section, we briefly describe a *robust state feedback* (RSFB) controller that uses the second information level. In the next Section, we analyze an *output feedback* (OFB) controller which uses the third information level. In Section V, we show simulations using controllers designed using all information levels for comparison purposes.

Lemma 1: Let the function $L(t) \in \mathbb{R}$ be defined as

$$L(t) := r^T(t) [g_{ij}^v(t) V_i(t) - \bar{u}_j(t)], \quad (17)$$

with $g_{ij}^v(t) = g_{ij}^v(s_{ij}(t), v_j(t))$ and $\bar{u}_j(t) \in \mathbb{R}^2$ given by

$$\bar{u}_j(t) := \beta \text{sign}(e_{ij}(t)), \quad (18)$$

where $\beta \in \mathbb{R}_{>0}$ is a control gain. If β satisfies

$$\beta > \left\| g_{ij}^v(t) V_i(t) \right\|_2 + \underline{k}_{12}^{-1} \left\| \frac{d[g_{ij}^v(t) V_i(t)]}{dt} \right\|_2,$$

with $\underline{k}_{12} := \lambda_{\min}(K)$ and K defined in (15). Then

$$\int_{t_0}^t L(\tau) d\tau < \zeta_b,$$

where the constant $\zeta_b \in \mathbb{R}_{>0}$ is defined as

$$\zeta_b := \beta \|e_{ij}(t_0)\|_1 - e_{ij}^T(t_0) g_{ij}^v(t_0) V_i(t_0), \quad (19)$$

and $\|\cdot\|_p$ denotes the \mathcal{L}_p norm, $p = 1, 2$.

Proof: The proof is omitted due to space limitations. ■

Theorem 1: Let the control law $\varpi_j(t)$ be defined as

$$\begin{aligned} \varpi_j(t) = & -g_{ij}^{-1}(s_{ij}, v_j) [\phi(\dot{s}_{ij}, s_{ij}, v_j) + 2K\dot{e}_{ij}(t) \\ & + K^2 e_{ij}(t) + \bar{u}_j(t)]. \end{aligned} \quad (20)$$

Then, the closed-loop system (16) is asymptotically stable, all its variables are bounded, and the tracking error and its derivative tend to zero with time.

Proof: Let the function $P(t) \in \mathbb{R}$ be defined as

$$P(t) := \zeta_b - \int_{t_0}^t L(\tau) d\tau \geq 0, \quad (21)$$

where $L(t)$ and ζ_b are defined in (17) and (19), respectively. Let the Lyapunov function candidate $W_1(t)$ be defined as

$$W_1(t) := \frac{1}{2} r^T(t) r(t) + P(t). \quad (22)$$

Taking time derivative of (22)

$$\dot{W}_1(t) = -r^T(t) K r(t) \leq -\underline{k}_{12} \|r(t)\|^2. \quad (23)$$

Therefore, $W_1(t) \in \mathcal{L}_\infty \cap \mathcal{L}_2$, then $r(t)$ and $P(t) \in \mathcal{L}_\infty \cap \mathcal{L}_2$. From definition (15), it is clear that $e_{ij}(t), \dot{e}_{ij}(t) \in \mathcal{L}_\infty$, and from (16), it can be seen that $\dot{r}(t), \dot{W}_1(t) \in \mathcal{L}_\infty$. Considering that $W_1(t)$ is lower bounded by $\|r(t)\|^2$, by the Barbalat's lemma and the Rayleigh-Ritz theorem $\dot{W}_1(t) \rightarrow 0$ and $r(t) \rightarrow 0$ as $t \rightarrow \infty$. Since (15) is a stable first order differential equations driven by $r(t)$, then $e(t), \dot{e}(t) \rightarrow 0$ as $t \rightarrow \infty$. ■

IV. OUTPUT FEEDBACK FORMATION CONTROL ALGORITHM (OFB)

In this Section, we describe and analyze the main contribution of this paper, an *output feedback* (OFB) controller. This controller uses only the specification $s_{ij}(t)$ and a high-gain observer (HGO) [15] to estimate the unknown state $\dot{s}_{ij}(t)$. Let the HGO be given by

$$\dot{\hat{s}}_1(t) = \hat{s}_2(t) + \frac{\alpha_1}{\varepsilon} (s_{ij}(t) - \hat{s}_1(t)), \quad (24)$$

$$\begin{aligned} \dot{\hat{s}}_2(t) = & -g_{ij}(s_{ij}, v_j) \varpi_j(t) - g_{ij}^s(s_{ij}, v_j) \hat{s}_2 \\ & + \frac{\alpha_2}{\varepsilon^2} (s_{ij}(t) - \hat{s}_1(t)), \end{aligned} \quad (25)$$

where $\alpha_1, \alpha_2 \in \mathbb{R}_{>0}^{2 \times 2}$, the HGO gains, are constant diagonal matrices, and $\varepsilon \in \mathbb{R}_{>0}$, the HGO constant, is designed such that $\hat{s}_1(t)$ and $\hat{s}_2(t)$ converge to the real values $s_{ij}(t)$ and $\dot{s}_{ij}(t)$ fast enough to stabilize the whole system.

Let the estimation error vector $\eta(t)$ be defined as $\eta(t) := [\eta_1^T(t), \eta_2^T(t)]^T \in \mathbb{R}^4$, with

$$\eta_1(t) = \frac{1}{\varepsilon} (s_{ij}(t) - \hat{s}_1(t)), \quad (26)$$

$$\eta_2(t) = \dot{s}_{ij}(t) - \hat{s}_2(t). \quad (27)$$

Using (24)-(27), the observer error dynamics become

$$\varepsilon \dot{\eta}(t) = A_0 \eta(t) + \varepsilon f(t), \quad (28)$$

where $A_0 = \begin{bmatrix} -\alpha_1 & I_2 \\ -\alpha_2 & 0_2 \end{bmatrix} \in \mathbb{R}^{4 \times 4}$ is a Hurwitz matrix, $0_2 \in \mathbb{R}^{2 \times 2}$ is the null matrix, $I_2 \in \mathbb{R}^{2 \times 2}$ is the identity matrix, and

$$f(t) = \begin{bmatrix} 0 \\ -g_{ij}^s(s_{ij}, v_j) \eta_2 - g_{ij}^v(s_{ij}, v_j) V_i(t) \end{bmatrix} \in \mathbb{R}^4.$$

If $\varepsilon \rightarrow 0$ and $d\tau = \frac{1}{\varepsilon} dt$ in (28), then

$$\frac{d\eta(\tau)}{d\tau} = A_0 \eta(\tau). \quad (29)$$

Equation (29) is called the *boundary layer system*.

Let the OFB controller be defined as

$$\begin{aligned} \varpi_j(t) = & -g_{ij}^{-1}(s_{ij}, v_j) [\phi(\hat{s}_2, s_{ij}, v_j) + 2K(\dot{\hat{s}}_{ij}^d(t) - \hat{s}_2(t)) \\ & + K^2 e_{ij}(t) + \bar{u}_j(t)]. \end{aligned} \quad (30)$$

Then, the closed-loop specification error dynamic model using the OFB control law (30) is

$$\begin{aligned} \dot{r}(t) = & -K r(t) - 2K \eta_2(t) + g_{ij}^s(s_{ij}, v_j) \eta_2(t) \\ & + g_{ij}^v(s_{ij}, v_j) V_i(t) - \bar{u}_j(t). \end{aligned} \quad (31)$$

Remark 1: The control signal $u_j(t)$ is saturated in order to avoid the *peaking phenomenon*.

Theorem 2: The control law (30) with the auxiliary control law (18) and the observer (24)-(25) ensure that the combined closed-loop system (28) and (31) is asymptotically stable.

Proof: The proof follows the guidelines of [16]. It is done in three steps: The first step proves that there exists an invariant set for the closed loop output feedback system based

on a composite Lyapunov function. The second step shows that any trajectory will be trapped into this invariant set in finite time if the HGO constant ε is chosen small enough. Third step demonstrates that this invariant set is globally uniformly ultimately bounded (GUUB).

Let $\mathcal{R} = \mathbb{R}^2$ be the region of attraction of the system (12)-(13) with the control law (20). Let \mathcal{D}_r be a compact set in the interior of \mathcal{R} . Let \mathcal{D}_c be defined by $\mathcal{D}_c := \{r(t) \in \mathcal{R} \mid W_1(t) \leq c\}$, where $W_1(t)$ is defined in (22) and $c > \max_{r \in \mathcal{D}_r} W_1(t)$ is a positive constant. The set \mathcal{D}_c is a compact subset of \mathcal{R} and \mathcal{D}_r is in the interior of \mathcal{D}_c .

For the boundary layer system, let $W_2(\eta)$ be defined as

$$W_2(\eta) := \eta^T P_0 \eta, \quad (32)$$

where $P_0 \in \mathbb{R}^{4 \times 4}$ is a positive definite matrix such that $P_0 A_0 + A_0^T P_0 = -I_4$, with A_0 defined in (29). Let the compact set \mathcal{D}_ε be defined by $\mathcal{D}_\varepsilon := \{\eta(t) \in \mathbb{R}^4 \mid W_2(t) \leq \rho \varepsilon^2\}$, where ρ is a positive constant to be selected later and ε is the HGO constant. Finally, let the set Σ_c be defined by $\Sigma_c := \mathcal{D}_c \times \mathcal{D}_\varepsilon$.

The derivative of (22) for $(e(t), \dot{e}(t), \eta(t)) \in \{W_1(t) = c\} \times \mathcal{D}_\varepsilon$ verifies

$$\begin{aligned} \dot{W}_1(t) &\leq -\underline{k}_{12} \left[\|r(t)\|^2 - \sigma_1 \|\eta(t)\| \right] \\ &\leq -\underline{k}_{12} (\mu - L_1 \varepsilon), \end{aligned} \quad (33)$$

with $\sigma_1 := \frac{\sigma_s + 2\underline{k}_{12}}{\underline{k}_{12}}$, $\sigma_s := \max_{s_{ij}, v_j} \|g_{ij}^s(s_{ij}, v_j)\|$, $\bar{k}_{12} := \lambda_{\max}(K)$, $\mu = \min_{r \in \partial \mathcal{D}_c} \{ \|r(t)\|^2 \}$, and $L_1 := \sigma_1 \sqrt{\frac{\rho}{\lambda_{\min}(P_0)}}$.

Analyzing the derivative of (32) for $(e(t), \dot{e}(t), \eta(t)) \in \mathcal{D}_c \times \{W_2(t) = \rho \varepsilon^2\}$ we find

$$\begin{aligned} \dot{W}_2(t) &\leq -\frac{\|\eta(t)\|^2}{2\varepsilon} [1 - 4\|P_0\| \sigma_s \varepsilon] \\ &\quad - \frac{\|\eta(t)\|}{2\varepsilon} [\|\eta(t)\| - 4\|P_0\| \sigma_v \varepsilon] \\ &\leq -\frac{\|\eta(t)\|^2}{2\varepsilon} (1 - 4\|P_0\| \sigma_s \varepsilon) \\ &\quad - \frac{\|\eta(t)\|}{2} \left(\sqrt{\frac{\rho}{\|P_0\|}} - 4\|P_0\| \sigma_v \right), \end{aligned} \quad (34)$$

with $\sigma_v := \max_{s_{ij}, v_j} \|g_{ij}^v(s_{ij}, v_j) V_i(t)\|$, and $\|P_0\| := \lambda_{\max}(P_0)$.

Taking $\rho = 16\sigma_v^2 \lambda_{\max}^3(P_0)$ and $\varepsilon_1 = \min\left(\frac{1}{4\sigma_s \|P_0\|}, \frac{\mu}{L_1}\right)$, for every $0 < \varepsilon \leq \varepsilon_1$, we have

$$\dot{W}_1(t) \leq 0,$$

for $(e(t), \dot{e}(t), \eta(t)) \in \{W_1(t) = c\} \times \mathcal{D}_\varepsilon$, and

$$\dot{W}_2(t) \leq 0,$$

for $(e(t), \dot{e}(t), \eta(t)) \in \mathcal{D}_c \times \{W_2(t) = \rho \varepsilon^2\}$. Therefore, $\Sigma_c := \mathcal{D}_c \times \mathcal{D}_\varepsilon$ is a positively invariant set.

Let the initial state satisfy $(e(0), \dot{e}(0), \eta(0)) \in \mathcal{D}_r \times \mathcal{Q}$, where \mathcal{Q} is a compact set such that $\mathcal{Q} \subseteq \mathbb{R}^4$. Using (26)-(27) it can be seen that

$$\|\eta(0)\| \leq \frac{c_3}{\varepsilon},$$

where $c_3 \in \mathbb{R}_{>0}$ is an appropriate constant. Because $(e(0), \dot{e}(0)) \in \mathcal{D}_r$, we have

$$\begin{aligned} \|e(t) - e(0)\| &\leq c_2^a t, \\ \|\dot{e}(t) - \dot{e}(0)\| &\leq c_2^b t, \\ \|r(t) - r(0)\| &\leq c_2 t, \end{aligned} \quad (35)$$

where $c_2^b, c_2^a, c_2 \in \mathbb{R}_{>0}$ are some positive constants. Therefore, there exists a finite time T_0 , independent of ε , such that $(e(t), \dot{e}(t)) \in \mathcal{D}_r$ for all $t \in [0, T_0]$. In consequence, if $t \in [0, T_0]$ and $W_2(\eta(t)) \geq \rho \varepsilon^2$, $W_2(t) \leq -\frac{1}{2\varepsilon} \|\eta(t)\|^2$ from (34). Then

$$\dot{W}_2(t) \leq -\frac{\mu_1}{\varepsilon} W_2(t), \quad (36)$$

with $\mu_1 := \frac{1}{2\|P_0\|}$. The solution for (36) is

$$W_2(t) \leq \frac{\mu_2}{\varepsilon^2} \exp\left(-\frac{\mu_1}{\varepsilon} t\right), \quad (37)$$

with $\mu_2 := c_3^2 \|P_0\|$. As it can be seen from (37), $\lim_{t \rightarrow \infty} W_2(t) = 0$. Let T_ε be the time for which $W_2(t)$ falls below to $\rho \varepsilon^2$, it must satisfy

$$W_2(\eta(T_\varepsilon)) \leq \frac{\mu_2}{\varepsilon^2} \exp\left(-\frac{\mu_1}{\varepsilon} T_\varepsilon\right) \leq \rho \varepsilon^2, \quad (38)$$

In consequence, $T_\varepsilon \geq \frac{\varepsilon}{\mu_1} \ln\left(\frac{\mu_2}{\rho \varepsilon^4}\right)$ and $\lim_{\varepsilon \rightarrow 0} T_\varepsilon = 0$. Then, it is possible to choose ε_2 small enough such that $T_\varepsilon = \frac{1}{2} T_0$, for all $\varepsilon \in (0, \varepsilon_2]$. It follows that $W_2(\eta(T_\varepsilon)) < \rho \varepsilon^2$ for all $\varepsilon \in (0, \varepsilon_2]$. Choosing $\varepsilon_1^* = \min(\varepsilon_1, \varepsilon_2)$, the trajectory $(e(t), \dot{e}(t), \eta(t))$ enters into the invariant set Σ_c in $t \in [0, T_\varepsilon]$ and remains in Σ_c , for all $t \geq T_\varepsilon$ and every $0 < \varepsilon \leq \varepsilon_1^*$. Moreover, the trajectory $(e(t), \dot{e}(t), \eta(t))$ is bounded by (35) and (37), for $t \in [0, T_\varepsilon]$ and $\varepsilon \in (0, \varepsilon_1^*]$.

If the initial state satisfy $(e(0), \dot{e}(0), \eta(0)) \in \mathcal{D}_r \times \mathcal{Q}$, then the trajectory of the system is inside Σ_c , for all $t \geq T_\varepsilon$ and $0 < \varepsilon \leq \varepsilon_1^*$. Because, from (37), $\lim_{\varepsilon \rightarrow 0} W_2(\eta(t)) = 0$, it is possible to find $\varepsilon_3 = \varepsilon_3(\delta_0) \leq \varepsilon_1^*$, for any given small value δ_0 , such that

$$\|\eta(t)\| \leq \frac{\delta_0}{2}, \quad (39)$$

for $t \geq T_{\varepsilon_3} = T_{\varepsilon_3}(\delta_0)$.

Let the compact sets \mathcal{D}_1 and \mathcal{D}_2 be given by

$$\mathcal{D}_1 := \{(e(t), \dot{e}(t)) \in \mathcal{R} : \|r(t)\|^2 \leq 2L_1 \varepsilon\}, \quad (40)$$

and

$$\mathcal{D}_2 := \{(e(t), \dot{e}(t)) \in \mathcal{R} : W_1(t) \leq v(\varepsilon)\}, \quad (41)$$

with $v(\varepsilon) := \max_{\|r\|^2 < 2L_1 \varepsilon} \{W_1(t)\}$. If $(e(t), \dot{e}(t)) \notin \mathcal{D}_1$,

$$\dot{W}_1(t) \leq -\frac{1}{2} \underline{k}_{12} \|r(t)\|^2.$$

Let $\varepsilon_4 = \varepsilon_4(\delta_0)$ be chosen such that \mathcal{D}_2 is in the interior of \mathcal{D}_c and

$$\mathcal{D}_2 \subset \left\{ (e(t), \dot{e}(t)) \in \mathcal{R} : \|e(t)\| \leq \frac{1}{4} \delta_0, \|\dot{e}(t)\| \leq \frac{1}{4} \delta_0 \right\}.$$

Then for all $(e(t), \dot{e}(t)) \in \mathcal{D}_c$, $(e(t), \dot{e}(t)) \notin \mathcal{D}_2$,

$$\dot{W}_1(t) \leq -\frac{1}{2} \underline{k}_{12} \|r(t)\|^2.$$

Therefore, the set $\Sigma_1 := \mathcal{D}_2 \times \mathcal{D}_\varepsilon$ is positively invariant and every trajectory in $\mathcal{D}_c \times \mathcal{D}_\varepsilon$ enters Σ_1 in finite time $T_{\varepsilon_4} = T_{\varepsilon_4}(\delta_0)$, for $\varepsilon \in (0, \varepsilon_4]$. Let $\varepsilon_2^* = \min\{\varepsilon_3, \varepsilon_4\}$ and $T_1 = \max\{T_{\varepsilon_3}, T_{\varepsilon_4}\}$, therefore

$$\|e(t)\| + \|\dot{e}(t)\| + \|\eta(t)\| \leq \delta_0, \quad (42)$$

with $\delta_0 > 0$, $\varepsilon \in (0, \varepsilon_2^*]$, and $t \geq T_1$. Then $(e(t), \dot{e}(t), \eta(t))$ is globally uniformly ultimately bounded (GUUB). ■

V. SIMULATION RESULTS

This section presents some simulations that validate the performance of the proposed controller. All simulations were written in C++ on a Linux platform using MPSLab, a motion planning, simulation, and virtual perception library [17].

Figures 3-7 show simulations of the proposed OFB controller with a 7-robot system. The initial positions are $q_\ell(0) = [0, -5, 0]^T$, $q_1(0) = [-3, -8, 0]^T$, $q_2(0) = [-3, -2, 0]^T$, $q_3(0) = [-3, -10, 0]^T$, $q_4(0) = [-3, -6, 0]^T$, $q_5(0) = [-3, -4, 0]^T$, and $q_6(0) = [-3, 0, 0]^T$. Their initial velocities are equal to 0.01. Figure 2 shows the specification for each robot. The inputs to the followers are saturated: $|v_j(t)| \leq 2.6$ and $|\omega_j(t)| \leq 11.5$. The sampling time is 10 msec. The parameters of the controllers are $k_1 = k_2 = 5.0$, $\beta = 4.0$, and we used the function

$$\bar{u}_j(t) := \beta \tanh(24.5e_{ij}(t)),$$

instead of (18) to avoid excessive chattering.

For comparison purposes, we include simulations with the RFSB controller (20) and with a critically damped *full-state feedback* (FSFB) controller that assumes full knowledge of the system

$$\begin{aligned} \varpi_j(t) = & -g_{ij}^{-1}(s_{ij}, v_j) [\phi(\dot{s}_{ij}, s_{ij}, v_j) + 2K\dot{e}_j(t) \\ & + K^2 e_{ij}(t) + g_{ij}^v(s_{ij}, v_j) V_i(t)]. \end{aligned} \quad (43)$$

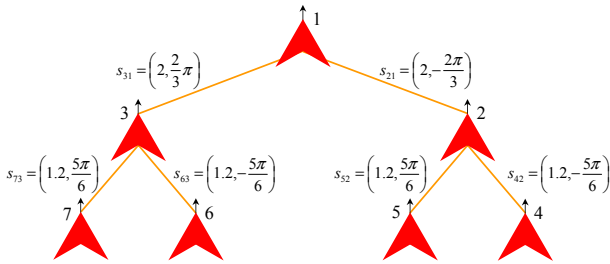


Fig. 2. Edge specification for 7 robots.

Figures 3-7 show simulation results when the leader follows a circular trajectory. The decentralized controller is able to drive each robot to the desired relative distance and desired bearing. Figure 3 shows the trajectories of seven robots using the OFB controller with $\varepsilon = 0.002$. Figures 4 and 5 show the decentralized control inputs and the specification error of follower 4 for the three controllers. It should be noted that not only the specification error, but also the control effort degrade with lack of knowledge. Notwithstanding, the behavior using the OFB controller is quite satisfactory.

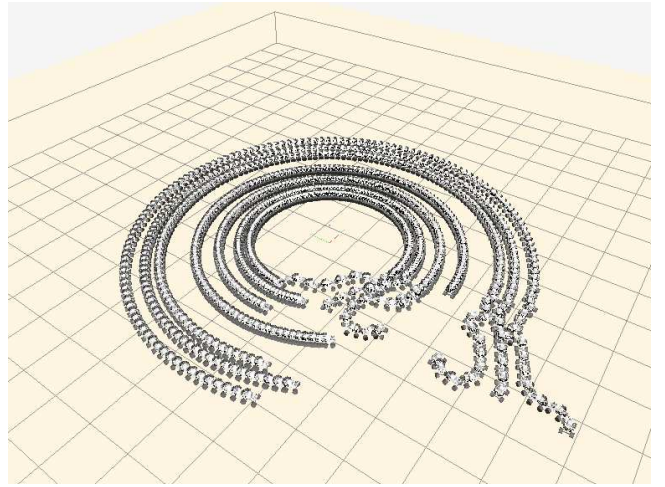


Fig. 3. Stroboscopic view of the simulation.

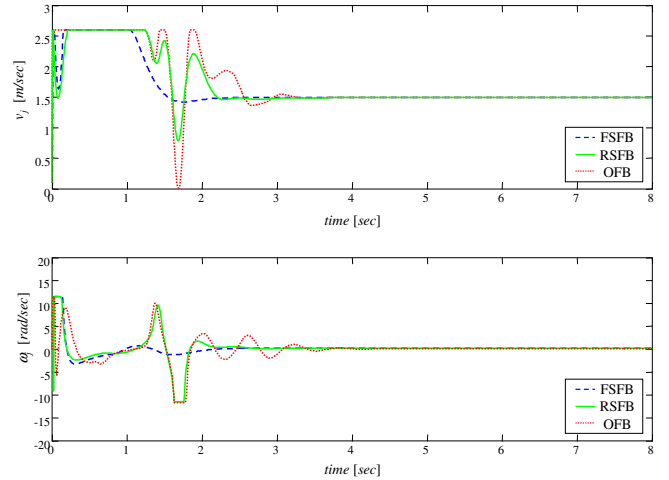


Fig. 4. Control inputs with controllers (43), (20), and (30).

Figures 6 and 7 illustrate the effects of the selection of the HGO constant ε on the control input and the specification error. As ε increases, specification errors increase mainly before the settling time, when the observer has not reached to steady state. However, the control effort decreases due to a more moderated peaking phenomenon.

VI. CONCLUSIONS

This paper presents a robust multi-vehicle output feedback decentralized controller. Using the main result of this work, each robot only requires a single camera to maintain a specified formation shape. The formation specification is given by the relative distance and bearing angle between each robot and its leader. A high gain observer is used to estimate the states of the robot and its neighbor(s).

A theoretical analysis based on Lyapunov stability theory has been performed to prove asymptotic stability of the system.

Simulations in a realistic 3D environment verify the performance of the output feedback controller. Currently, the multi-vehicle decentralized control methodology is being tested on actual car-like mobile robots. Future research will focus on

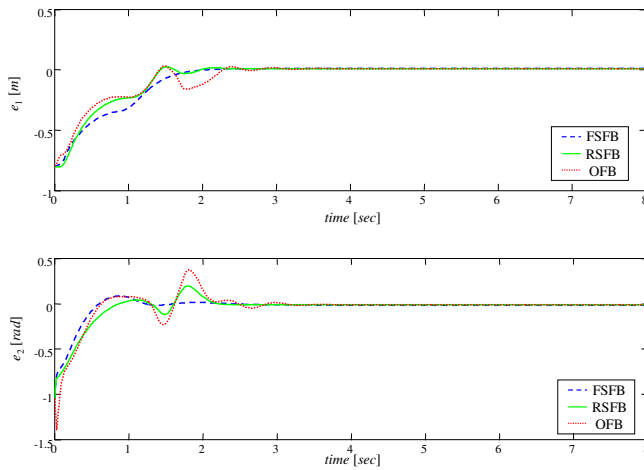


Fig. 5. Output errors with controllers (43), (20), and (30).

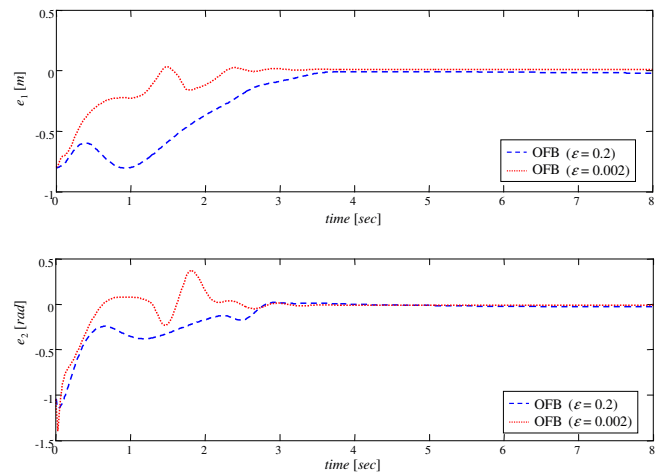


Fig. 7. Output errors with $\varepsilon = 0.2$ and $\varepsilon = 0.002$.

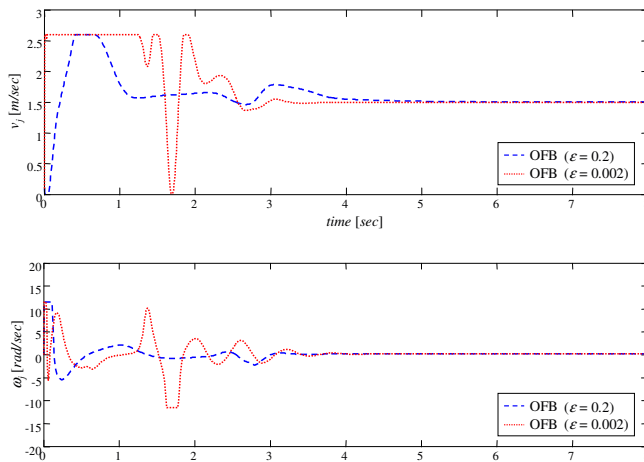


Fig. 6. Control inputs with $\varepsilon = 0.2$ and $\varepsilon = 0.002$.

the analysis of input-to-state (ISS) properties of this controller/observer pair, the effects of formation reconfiguration on the connectivity of the formation control, and communication graphs.

ACKNOWLEDGMENT

The authors would like to thank Dr. Tony Zhang for helpful discussions on the formulation of the output feedback controller. This work is supported in part by NSF grants #0311460 and CAREER #0348637 and by the U.S. Army Research Office under grant DAAD19-03-1-0142 (through the University of Oklahoma.)

REFERENCES

- [1] R. Fierro, L. Chaimowicz, and V. Kumar, "Multi-robot cooperation," in *Autonomous Mobile Robots: Sensing, Control, Decision Making and Applications*, S. Ge and F. Lewis, Eds. CRC Press - Taylor & Francis Group, 2005, ch. 11, to appear.
- [2] J. Bellingham, M. Tillerson, M. Alighanbari, and J. How, "Cooperative path planning for multiple UAVs in dynamic and uncertain environment," in *Proceedings of the IEEE Conference on Decision and Control*, no. 3, Las Vegas, NV, Dec. 2002, pp. 2816–2822.
- [3] J. Ousingsawat and M. Campbell, "Establishing optimal trajectories for multi-vehicle reconnaissance," in *Proceedings of the AIAA Guidance, Navigation and Control Conference*, Providence, RI, Aug. 2004, (CD-ROM).

- [4] S. Zelinski, T. Koo, and S. Sastry, "Optimization-based formation reconfiguration planning for autonomous vehicles," in *Proceedings of the IEEE International Conference on Robotics and Automation*, Taipei, Taiwan, Sept. 2003, pp. 3758–3763.
- [5] A. Jadbabaie, J. Lin, and A. Morse, "Coordination of groups of mobile autonomous agents using nearest neighbor rules," *IEEE Transactions on Automatic Control*, vol. 48, no. 6, pp. 988–1001, June 2003.
- [6] N. Moshtagh, A. Jadbabaie, and K. Daniilidis, "Vision-based distributed coordination and flocking of multi-agent systems," in *Proceedings of Robotics: Science and Systems*, Cambridge, USA, June 2005.
- [7] G. Lafferriere, A. Williams, J. Caughman, and J. Veerman, "Decentralized control of vehicle formations," *Systems & Control Letters*, vol. 54, no. 9, pp. 899–910, Sept. 2005.
- [8] X. Chen, A. Serrani, and H. Özbay, "Control of leader-follower formations of terrestrial uavs," in *Proceedings of the 42nd IEEE Conference on Decision and Control*, no. 1, Maui, Hawaii USA, Dec. 2003, pp. 498–503.
- [9] R. Vidal, O. Shakernia, and S. Sastry, "Formation control of nonholonomic mobile robots with omnidirectional visual servoing and motion segmentation," in *Proceedings of the IEEE International Conference on Robotics and Automation (ICRA 03)*, no. 1, Taipei, Taiwan, Sept. 2003, pp. 584–589.
- [10] N. Cowan, O. Shakerina, R. Vidal, and S. Sastry, "Vision-based follow-the-leader," in *Proceedings of the 2003 IEEE/RSJ International Conference on Intelligent Robots and Systems (IROS 2003)*, no. 2, Las Vegas, Nevada USA, Oct. 2003, pp. 1796–1801.
- [11] C.-P. Tang, R. Bhatt, and V. Krovvi, "Decentralized kinematic control of payload by a system of mobile manipulators," in *Proceedings of the 2004 IEEE International Conference on Robotics and Automation*, no. 3, New Orleans, LA USA, Apr. 2004, pp. 2462–2467.
- [12] B. Gerkey and M. Mataric, "Pusher-watcher: an approach to fault-tolerant tightly-coupled robot coordination," in *Proceedings of the IEEE International Conference on Robotics and Automation*, no. 1, Washington, DC, May 2002, pp. 464–469.
- [13] R. Diestel, *Graph Theory*. New York: Springer-Verlag, 2000.
- [14] H. Tanner, G. Pappas, and V. Kumar, "Leader-to-formation stability," *IEEE Transactions on Robotics and Automation*, vol. 20, no. 3, pp. 443–455, June 2004.
- [15] H. Khalil, *Nonlinear Systems*, 3rd ed. Prentice Hall, Upper Saddle River, NJ, 2002.
- [16] A. Atassi and H. Khalil, "A separation principle for the stabilization of a class of nonlinear systems," *IEEE Transactions on Automatic Control*, vol. 44, no. 9, pp. 1672–1687, Sept. 1999.
- [17] O. Orqueda, J. Figueroa, and O. Agamennoni, "Motion planning and control: From virtual environments to the real world," in *Proceedings of the IFAC International Symposium on Intelligent Components and Instruments for Control Applications (SICICA)*, Aveiro, Portugal, July 2003.